Construction and Building Materials 169 (2018) 132–141

Contents lists available at ScienceDirect

Construction and Building Materials

journal homepage: www.elsevier.com/locate/conbuildmat

Probabilistic-based characterisation of the mechanical properties of CFRP laminates

S. Gomes [a], D. Dias-da-Costa [b,a,*], L.A.C. Neves [c], S.A. Hadigheh [b], P. Fernandes [d], E. Júlio [e]

[a] ISISE, Department of Civil Engineering, University of Coimbra, Rua Luís Reis Santos, 3030-788 Coimbra, Portugal
[b] School of Civil Engineering, The University of Sydney, Sydney, NSW 2006, Australia
[c] Resilience Engineering Research Group, University of Nottingham, Faculty of Engineering, University Park, United Kingdom
[d] Civil Engineering Department, Instituto Politécnico de Leiria, Portugal
[e] CEris-ICIST, DECivil, Instituto Superior Técnico, Universidade de Lisboa, Av. Rovisco Pais, 1049-001 Lisboa, Portugal

HIGHLIGHTS

- Very limited data exists on non-deterministic models for FRPs.
- Past studies used small sample sizes and ignored the tail. Hence, may be inaccurate.
- New models given for the mechanical properties of FRPs using an extensive database.
- Validation performed in the tail region, models suitable for reliability analysis.

ARTICLE INFO

Article history:
Received 1 August 2017
Received in revised form 15 February 2018
Accepted 25 February 2018
Available online 3 March 2018

Keywords:
CFRP laminates
Strengthening of structures
Mechanical properties
Probabilistic models

ABSTRACT

Fibre reinforced polymer (FRP) composites have been increasingly used worldwide in the strengthening of civil engineering structures. As FRP becomes more common in structural strengthening, the development of probability-based limit state design codes will require accurate models for the prediction of the mechanical properties of the FRPs. Existing models, however, are based on small sample sizes and ignore the importance of the tail region for analyses and design. Addressing these limitations, this paper presents a probabilistic-based characterisation of the mechanical properties of carbon FRP (CFRP) laminates using a large batch of tension tests. The analysed specimens were pre-cured laminates of carbon fibres embedded in epoxy matrices, which is the most commonly used laminate for the strengthening concrete beams and slabs. Based on the existing data, probabilistic models and correlations were established for the Young's modulus, ultimate strain and tensile strength. Analyses demonstrate the suitability of the Weibull distribution for the estimation of CFRP properties. Results also show that the statistical characterisation of the mechanical properties should be performed with a focus on the tail region. The proposed distributions constitute a set of validated probabilistic models that can be used for performing reliability analyses of structures strengthened with CFRP laminates.

1. Introduction

During the last decades, externally bonded reinforcement (EBR) of fibre-reinforced polymers (FRP) has become a common technique to strengthen and upgrade civil engineering structures. FRP is usually used in the form of wet lay-up sheets or pre-fabricated laminates due to their simplicity and lower capital cost. The former system is based on the direct application of fibre sheets saturated with resin, whereas the second uses pre-fabricated cured strips. There are also automated techniques using vacuum (e.g. resin infusion techniques) or vacuum and heat (e.g. heated vacuum bag only) for impregnation of fibres [1–3]. The characteristics of the FRP, namely its lightweight, high durability in aggressive environments, ease of installation and cost effectiveness, are quite competitive for strengthening purposes and constitute a good alternative to more traditional methods and materials, such as EBR using steel plates or concrete jacketing [1]. There are several examples where FRPs were used to increase the flexural, shear or axial capacity of structural members, such as beams, slabs, columns, or joints [4–8].

* Corresponding author.
E-mail address: daniel.diasdacosta@sydney.edu.au (D. Dias-da-Costa).

https://doi.org/10.1016/j.conbuildmat.2018.02.190
0950-0618/

The growing interest in FRP composites resulted in the development of several design guidelines (e.g. CEB-FIB [9], TR-55 [10], CNR [11] and ACI 440.2R-08 [12]). These, however, are not presently at a level of development comparable to those used in structural concrete and steel design. Considering the uncertainties present in FRP applications, new guidelines are required to develop probability-based limit state design codes and to support the acceptance of FRP materials in civil engineering [13,14]. Despite previous reliability studies (e.g. Ellingwood [13], Plevris, Triantafillou [15], Okeil, El-Tawil [16], Monti and Santini [17], Atadero, Lee [18], Atadero and Karbhari [19], Okeil, Belarbi [20], and Ali, Bigaud [21]) having addressed some of these uncertainties, the statistical information is still limited in the development of more accurate probabilistic models.

A variety of factors affect the properties of FRP after manufacturing which create a degree of uncertainty and must be considered in design [22]. Atadero [23] employed normal, log-normal, Weibull and Gamma distributions to analyse the probabilistic properties of field-manufactured wet lay-up carbon and glass composites. Six sets, composed by one, three or four subsets resulting in 903 samples, were considered to assess the tensile strength, the Young's modulus and the laminate thickness. Despite the large number of samples used, the need to divide them in smaller subsets of different properties and manufacturing processes led to a significant reduction in the sample size available for the statistical analysis. From this study, the Weibull distribution was proposed to model the tensile strength, whereas the Young's modulus and the laminate thickness were modelled using a log-normal distribution. Zureick, Bennett [24] performed statistical analysis on over 600 samples of pultruded composite materials fabricated from E-glass fibres and polyester or vinylester matrices. However, due to the differences in the properties of the specimens, each subset contained no more than 30 samples. Zureick, Bennett [24] investigated the longitudinal tensile and compressive strengths, the longitudinal tensile and compressive modulus, the shear strength and modulus. The Weibull distribution was proposed to model the strength and stiffness properties. Further studies on the probabilistic properties of composites can be found in Jeong and Shenoi [25] or Lekou and Philippidis [26].

2. Research significance

The main limitations in previous studies are mainly related with the small number of samples available which could compromise the characterisation of the probabilistic distributions. Previous models focused on the entire sample distribution and ignored the importance of the tail region for probabilistic analysis. It is also difficult to obtain suitable probability distribution functions without sufficient number of samples and to output accurate estimates for the tail region. As such, discrepancy between existing models and experimental data could reach several orders of magnitude [27]. To address these limitations, the main aim of this work is to validate and propose probabilistic models for the mechanical properties of the carbon FRP (CFRP) laminates (i.e. Young's modulus, ultimate strain and tensile strength) and to highlight the importance of the tail of the sample distribution. All statistical analyses are performed on a large and homogeneous batch of samples.

3. Experimental tests

The data used in the present study concerns pultruded laminates produced from the same manufacturer. The CFRP had a density of 1.4 g/cm^3 and a fibre content above 68% in volume, with a tensile design stress of 1000 MPa and 1300 MPa, respectively for 0.6% and 0.8% elongation. As part of the quality process of the manufacturer, the mechanical properties of the CFRP were consistently assessed in the fibre direction. In total, a large set of 1368 coupon samples were obtained for this process, collected from specimens with various cross sections (60–168 mm^2) – see Appendix A for complete sample characterisation.

The coupon configuration for tensile testing was based on the EN ISO 527-5 [28] standard (Table 1), with all the tensile tests being carried out according to same standard on a Zwick Z100 universal testing machine (Fig. 1a). As part of the experimental procedure, a pre-load of 0.1 kN was applied to avoid any misalignment within the system. Then, each coupon sample was loaded at a constant displacement rate of 2 mm/min until failure. Both loading and CFRP strain were directly measured using a load cell and a strain gauge, respectively (Fig. 1b).

It should be denoted that the pre-load was considered in the analyses described in the following sections. Furthermore, the data for statistical analysis was carefully selected to exclude invalid results arising from: (i) tab region failure; (ii) broken fibres in contact with the strain gauge; (iii) slippage of specimens from the jaws; and (iv) failure of specimens at or close to the jaws. The stress versus strain curves were plotted, and the tensile strength, modulus of elasticity, and ultimate strain of the FRP were calculated. Fig. 2 illustrates typical raw stress-strain diagrams for coupon samples tested where the linear elastic behaviour can be observed nearly up to failure.

4. Statistical models

Three statistical distributions were considered to model the CFRP properties: (i) normal; (ii) log-normal; and (iii) Weibull. The probability density function (PDF) and the cumulative distribution function (CDF) for each distribution were obtained from the following relationships.

- Normal distribution

$$\text{PDF}: \quad f(x|\mu,\sigma) = \frac{1}{\sigma\sqrt{2\pi}} e^{-\frac{1}{2}\left(\frac{x-\mu}{\sigma}\right)^2}, \quad \sigma > 0, \quad -\infty < x, \quad \mu < +\infty, \tag{1}$$

$$\text{CDF}: \quad F(x|\mu,\sigma) = \frac{1}{\sqrt{2\pi}} \int_{-\infty}^{x} e^{-\frac{1}{2}\left(\frac{t-\mu}{\sigma}\right)^2} dt, \tag{2}$$

where μ is the mean and σ is the standard deviation, and t is a real variable.

- Log-normal distribution

$$\text{PDF}: \quad f(x|\mu,\sigma) = \frac{1}{x\sigma\sqrt{2\pi}} e^{-\frac{(\ln x-\mu)^2}{2\sigma^2}}, \quad x > 0, \quad \sigma > 0, \quad -\infty < \mu < +\infty, \tag{3}$$

$$\text{CDF}: \quad F(x|\mu,\sigma) = \frac{1}{\sigma\sqrt{2\pi}} \int_{0}^{x} \frac{1}{t} e^{-\frac{1}{2}\left(\frac{\ln t-\mu}{\sigma}\right)^2} dt. \tag{4}$$

Table 1
Details of the tensile samples based on EN ISO 527-5 [28].

Detail	Values (mm)
FRP length	250
FRP width	15 (±0.5)
FRP thickness	1.0 (±0.2)
Tab extension	>50
Tab thickness	0.5–2
Grip extension	≥7
Gauge length	50 (±1)
Bevel angle	90

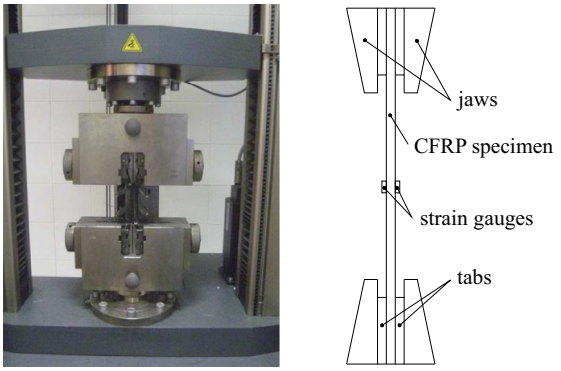

Fig. 1. Experimental test set-up: (a) testing machine (courtesy of S&P Clever Reinforcement Ibérica); (b) instrumentation.

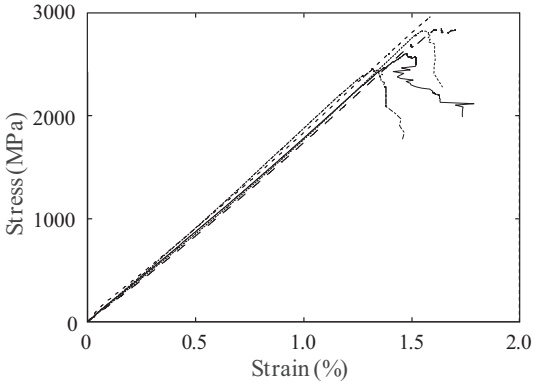

Fig. 2. Raw stress-strain diagrams for five tested coupon samples.

- Weibull distribution

Since previous studies [29] showed that the statistical characterisation of the CFRP does not improve using a three-parameter Weibull distribution, a two-parameter approach was adopted here. This is defined by the following expressions:

$$\text{PDF}: \quad f(x|\alpha,\beta) = \frac{\alpha}{\beta}\left(\frac{x}{\beta}\right)^{\alpha-1} e^{-\left(\frac{x}{\beta}\right)^{\alpha}}, \quad \alpha,\beta \geq 0, \quad 0 \leq x < +\infty, \tag{5}$$

$$\text{CDF}: \quad F(x|\alpha,\beta) = 1 - e^{-\left(\frac{x}{\beta}\right)^{\alpha}}, \tag{6}$$

where α and β are the shape and the scale parameters, respectively.

The best-fit distributions were found following the censored maximum likelihood estimation (MLE) [30]. This method allows estimating parameters θ of a statistical distribution for a sample, considering the following:

$$L(\theta|\hat{x}_1,\hat{x}_2,\ldots,\hat{x}_n) = \prod_{i=1}^{n} f_X(\hat{x}_i|\theta), \tag{7}$$

in which $L(.)$ is the likelihood that the parameters $\theta = \theta_1,\theta_2,\ldots,\theta_n$ properly describe the sample $\hat{x} = \hat{x}_1,\hat{x}_2,\ldots,\hat{x}_n$, and f_X is the joint PDF of a sample. The maximum likelihood estimators are computed from the set of parameters that maximise the likelihood function by considering all possible cases of θ.

Since the tail region is critical for structural reliability analysis and prediction, especial attention is given to this region in the statistical analysis of the tensile tests. The adopted technique considers explicitly the values of the lower tail that are smaller than a predefined bound, whereas the remaining values are used implicitly [31]. The censored MLE can be defined as follows:

$$L = L1 \times L2, \tag{8}$$

with

$$L1 = \prod_{i=1}^{j} f(x_i|\theta), \tag{9}$$

$$L2 = P(X \geq x_G|\theta)^{n-j}, \tag{10}$$

$$P(X \geq x_G|\theta) = 1 - F(x_G|\theta), \tag{11}$$

where $L1$ is the likelihood associated with the j observations of values equal or lower than the bound value x_G. $L2$ is the likelihood associated with the observations of values higher than the bound value x_G. $F(x_G|\theta)$ is the CDF of x_G given the PDF θ, n is the total number of observations and $n-j$ is the total number of observations exceeding the bound value x_G. The best fit can be computed iteratively through the optimisation problem of maximising L.

For each property, the distributions families were adjusted for the entire sample and the lower percentiles of: 20th, 25th, 30th, 35th and 40th. The 20th percentile is considered to be a reasonable choice for reliability studies in this research, since it includes the region of interest without decreasing the sample size to statistically meaningless values.

The goodness of fit for all distributions was examined using the Anderson-Darling test for the: (i) entire samples; and (ii) samples with right-censored data. The Anderson-Darling test was adopted since it provides adequate comparison tools for tail regions [32]. The statistic for the right-censored data and entire data can be obtained respectively by [33]:

$$A^2 = -\frac{1}{n}\sum_{i=1}^{r}(2i-1)\left[\ln Z_{(i)} - \ln(1 - Z_{(n+1-i)})\right] - n, \tag{12}$$

$$A^2_{r,n} = -\frac{1}{n}\sum_{i=1}^{r}(2i-1)\left[\ln Z_{(i)} - \ln\{1 - Z_{(i)}\}\right] - 2\sum_{i=1}^{r}\ln\{1 - Z_{(i)}\} - \frac{1}{n}\left[(r-n)^2\ln\{1 - Z_{(r)}\} - r^2\ln Z_{(r)} + n^2_{(r)}\right], \tag{13}$$

where r is the uncensored observation, n is the total number of observations and Z denotes the CDF of the probability distribution. The statistic values (A^2) were then compared with the critical values (CV) presented by Stephens and D'Agostino [33]. The null hypothesis ($H0$) of the data following the distribution tests was not rejected if the statistic value was lower than the critical value. The critical values for different percentiles are given in Table 2. To minimise Type I errors, which occur when $H0$ was wrongly rejected, or Type II errors, in which $H0$ was wrongly accepted, the significance level (α) was set at 10%.

4.1. Young's modulus

The Young's modulus is one of the significant parameters related with the structural safety of the FRP for rehabilitation of structures, particularly in situations where failure is expected to occur at tensile stresses significantly lower than the ultimate strength of the FRP. This type of failure usually occurs when debonding of the CFRP or concrete crushing are the dominant failure mechanisms [9].

The best fit for each PDF for the Young's modulus is illustrated in Fig. 3. As it can be seen in Fig. 3a, when the distributions were fitted to the entire sample, significant differences existed in the range of the lower and upper values. Considering the importance of the tail regions in safety assessment, clear improvements were

Table 2
Critical values for different percentiles.

Percentile	20%	25%	30%	35%	40%	100%
CV	0.436	0.545	0.651	0.756	0.857	1.933

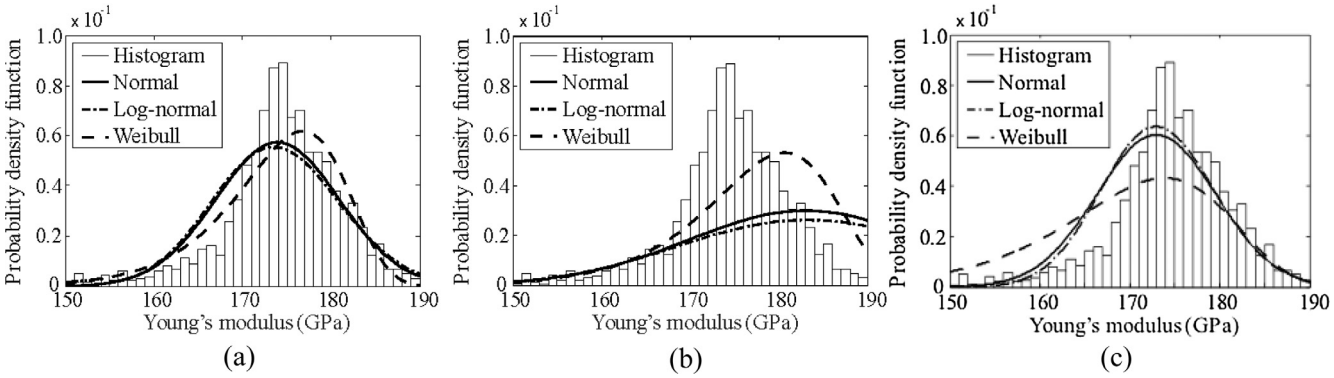

Fig. 3. PDF for the Young's modulus of: (a) the entire data fit, (b) the 20th percentile lower tail fit; and (c) the 20th percentile upper tail fit.

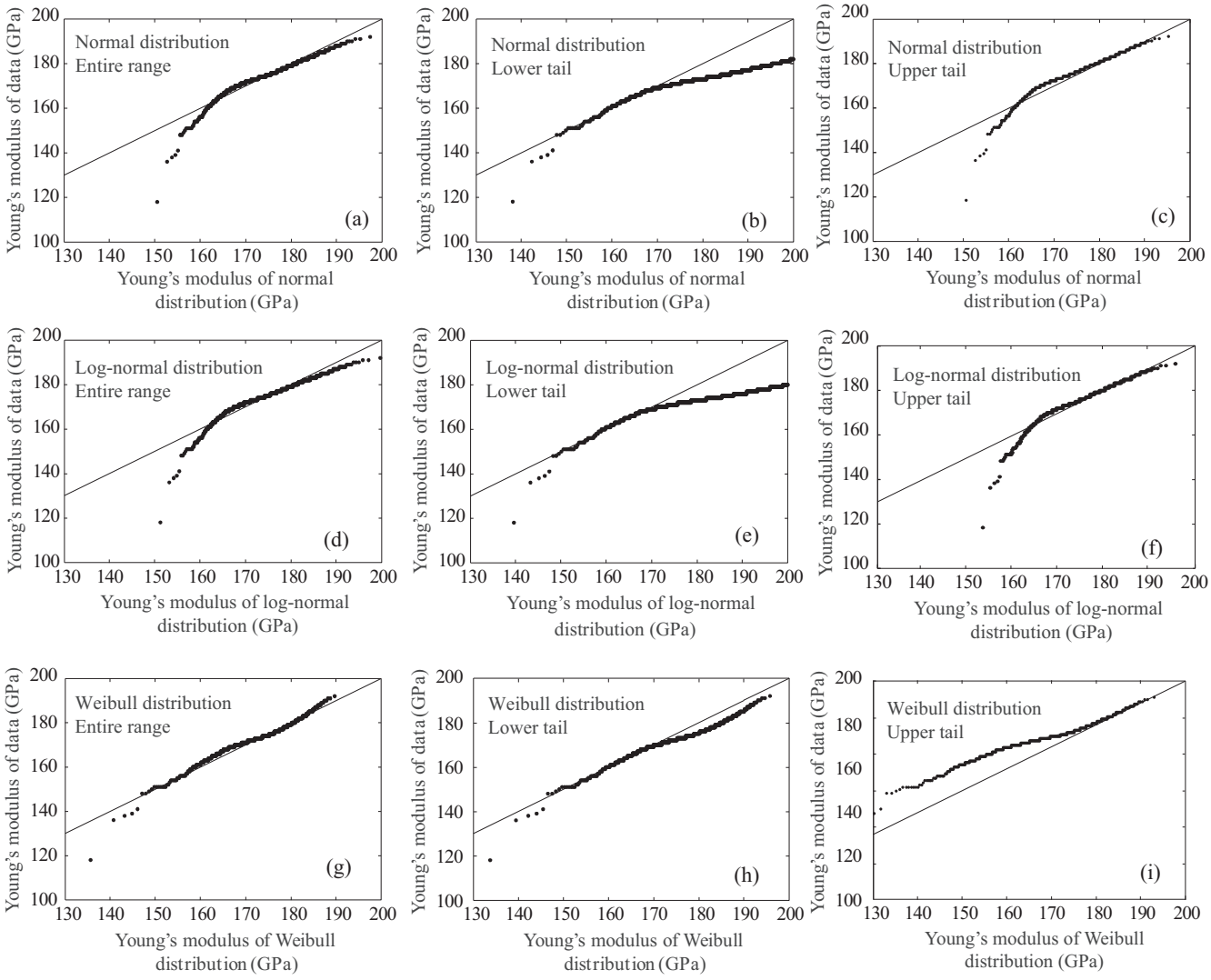

Fig. 4. Q-Q plot of the Young's modulus based on: normal distribution adjusted to (a) the entire range, and (b) the 20th lower and (c) 20th upper percentile; log-normal distribution adjusted to (d) the entire range, and (e) the 20th lower and (f) 20th upper percentile; and Weibull distribution adjusted to (g) the entire range, and (h) the 20th lower and (i) 20th upper percentile.

Table 3
Statistical values for the Anderson-Darling goodness of fit test for each percentile and distribution.

Percentile	Normal	Log-normal	Weibull
20%	0.279	0.373	0.123
25%	0.598	0.696	0.427
30%	1.587	1.697	1.327
35%	1.587	1.697	1.327
40%	4.226	4.351	3.767
100%	18.236	23.568	13.678

achieved by applying the approach described above firstly to the lower 20th percentile region – see Fig. 3b. Both normal and log-normal distributions provided similar results, whereas the Weibull distribution showed the closest fit to the data. For more clarity, the Q-Q curves were plotted for three distributions in Fig. 4. The Weibull distribution was able to approximate the experimental data with high precision in both 20th percentile lower tail and entire range regions (Fig. 4e and f).

The statistic values for the Anderson-Darling goodness of fit test are presented in Table 3. In this table, the shaded cells refer to tests where the distributions were not rejected. The results showed that the Weibull was the only distribution where the null hypothesis was not rejected for the highest percentile (in this case the 25th). Additionally, this distribution presented the smallest statistical values, meaning that the average squared distance between the data and the fitted distribution was also the lowest.

Based on the statistical analysis of the experimental data, the following shape and scale parameters were proposed to model the Young's modulus based on the Weibull distribution adjusted to the 20th percentile:

$$E_f \sim \mathrm{W}(26.2, 180.9)\mathrm{GPa} \tag{14}$$

Depending on the design situation, the upper percentile of the Young's modulus might also be required. For example, in situations of debonding failure, an higher value for this material parameter can provide more conservative estimates on the capacity of the structural member. For this reason, the study described in this section was similarly applied to obtain the best fit distribution for the 20th upper percentile. Results are shown in Figs. 3 and 4, whereas the Weibull distribution adjusted to the upper tail region was given by the following equation:

$$E_f \sim \mathrm{W}(20.4, 174.4)\mathrm{GPa}. \tag{15}$$

Using the distributions shown in Eqs. (14) and (15), the characteristic values for the Young's modulus were determined as 161.5 GPa and 184.0 GPa, respectively corresponding to the 5th and 95th percentiles. It should be mentioned that the lower value was only slightly below the design value provided by the manufacturer (165 GPa). Results also showed that the coefficient of variation was reduced, i.e., 0.04.

4.2. Ultimate strain

The ultimate strain of the FRP is another important parameter in structural safety since the material typically exhibits elastic behaviour until failure. The same procedure described above was followed to analyse this material parameter from the tensile tests. Conversely to what was observed for the Young's modulus, the statistical analysis showed that (Fig. 5a) none of the selected distributions could fit well the lower tail when using the entire sample. Fig. 5b shows the ultimate strain probability density functions adjusted to the lower tail, where the Weibull distribution was the one that provided the best results. The same trend could be seen in the corresponding Q-Q plots illustrated in Fig. 6.

The Anderson-Darling goodness of fit test presented in Table 4 shows that the Weibull was the only distribution not rejected for the highest percentile (in this case the 40th), whereas the null hypothesis was rejected for all the distributions adjusted to the entire sample. Based on these results, the Weibull distribution adjusted to the 20th percentile was proposed to model the ultimate strain with a coefficient of variation of 0.06, and the following parameters:

$$\varepsilon_{fu} \sim \mathrm{W}(17.1, 1.5)\%. \tag{16}$$

4.3. Tensile strength

The tensile strength of the FRP is important in situations where failure occurs within the laminate. This can be particularly critical for prestressed FRP laminates, since the prestress loading often represents a high percentage of the tensile strength [34,35]. Preliminary results of the distributions adjusted to the entire sample showed that all selected distributions were unable to provide a good fit in the lower tail, as illustrated in Fig. 7a. An improvement could be obtained when the procedure based on fitting the CDF to the lower tail is followed – see Fig. 7b. The Weibull distribution performed better in both cases.

The Q-Q plots showed the similarity between normal and log-normal distributions – see Fig. 8a–d and that using the entire

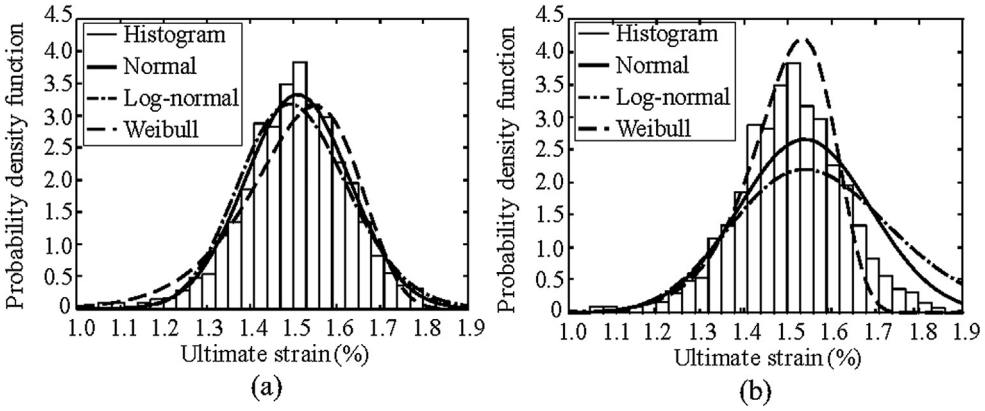

Fig. 5. PDF for the ultimate strain of the entire data fit (a) and 20th percentile lower tail fit (b).

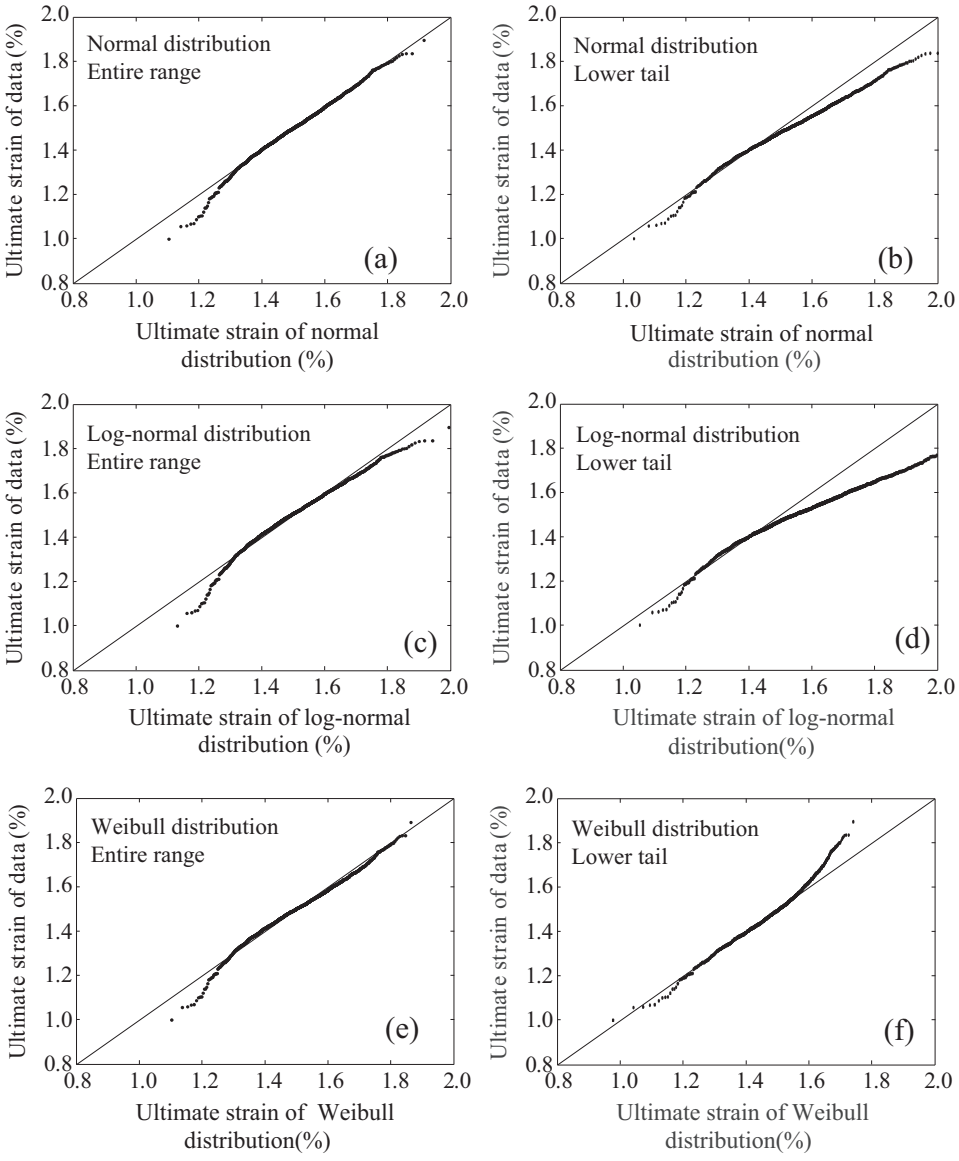

Fig. 6. Q-Q plot of the ultimate strain based on: normal distribution adjusted to (a) the entire range and (b) the lower tail; log-normal distribution adjusted to (c) the entire range and (d) the 20th lower percentile; and Weibull distribution adjusted to (e) the entire range and (f) the 20th lower percentile.

Table 4
Statistical values for the Anderson-Darling goodness of fit test for each percentile and distribution.

Percentile	Normal	Log-normal	Weibull
20%	0.206	0.351	0.050
25%	0.237	0.393	0.057
30%	0.433	0.656	0.101
35%	0.771	1.148	0.126
40%	1.371	2.056	0.136
100%	2.5453	5.485	8.9873

sample was not suitable for the lower tail region. The good fit obtained with the Weibull distribution in this region can be noticed by comparing Fig. 8e and f. Despite these observations, the goodness of fit results for the lowest tail fit (Table 5) did not reject any of the distributions for the 20th and 25th percentiles. However, since the Weibull presented a better result than the other models overall, it was adopted here as the distribution model for the tensile strength with the following parameters:

$$f_f \sim \mathrm{W}(15.9, 2777.0)\mathrm{MPa}. \quad (17)$$

The 5th characteristic value using the proposed distribution was 2304.2 MPa, which was only 0.3% higher than the experimental value (2299.0 MPa). The coefficient of variation was also very small, i.e. 0.08. The selected distribution is in agreement with the works from Atadero [23] and Zureick, Bennett [24] for prediction of the tensile strength based on the entire data fit.

5. Correlation analysis

This section presents a correlation analysis on the mechanical properties discussed in the previous section. Within the linear elastic range, strain, stress and Young's modulus are naturally related with each other by the Hooke's law. When approaching ultimate values – i.e. the material strength – the standard relation may no longer hold and more suitable relationships may need to be

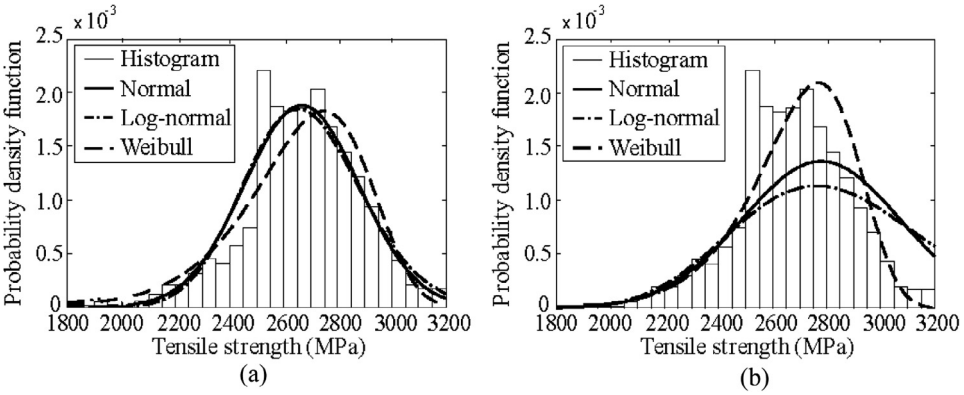

Fig. 7. PDF for the tensile strength of (a) the entire data fit (b) and the 20th percentile lower tail fit.

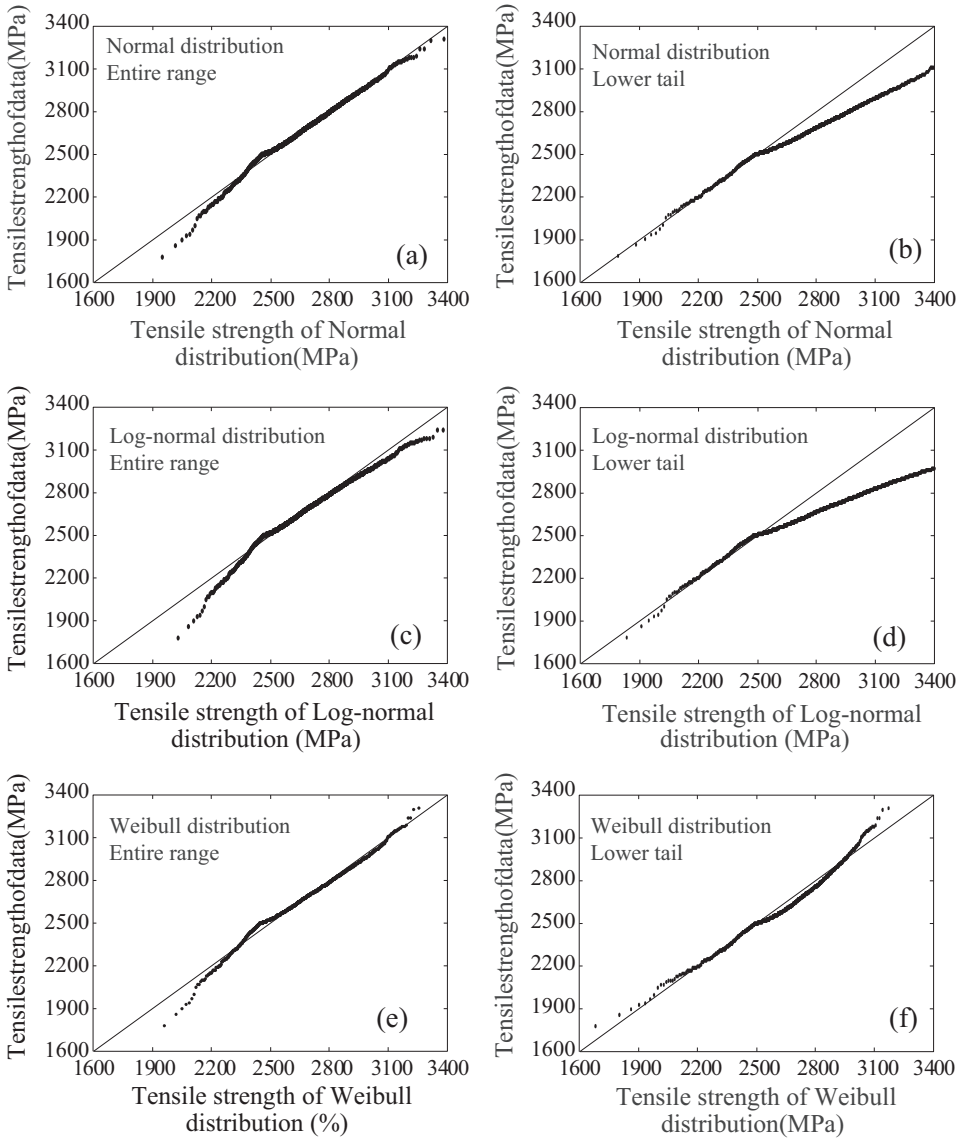

Fig. 8. Q-Q plot of the tensile strength based on: normal distribution adjusted to (a) the entire range and (b) the lower tail; log-normal distribution adjusted to (c) the entire range and (d) the 20th lower percentile; and Weibull distribution adjusted to (e) the entire range and (f) the 20th lower percentile.

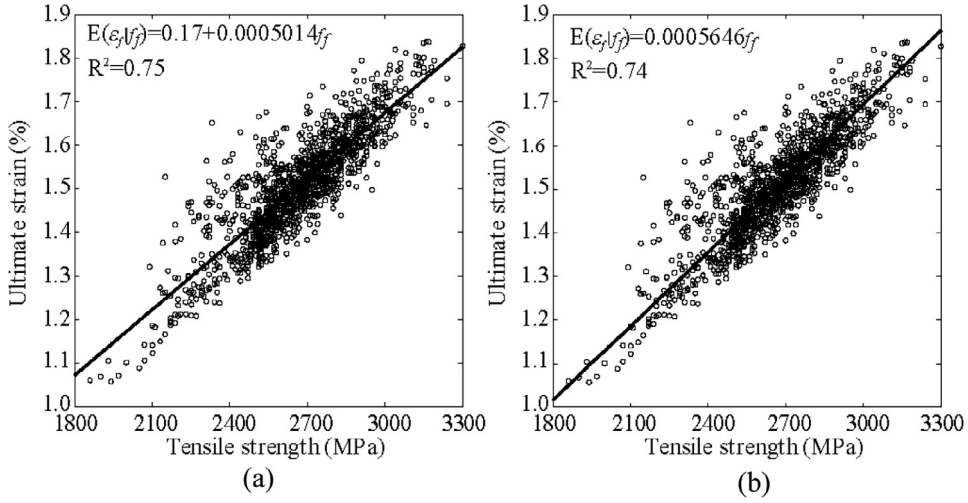

Fig. 9. Scatter diagram of tensile strength versus ultimate strain of (a) the regression without constraints and (b) the regression across the origin.

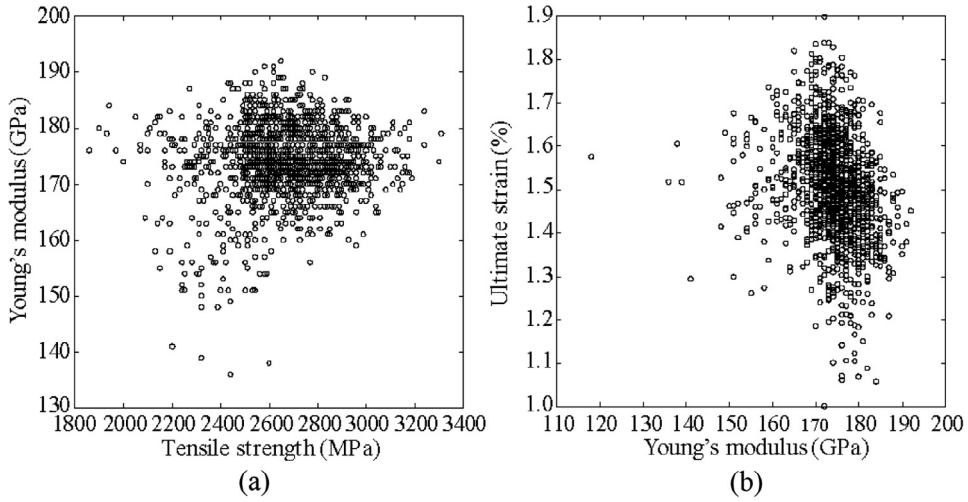

Fig. 10. Scatter diagram of (a) tensile strength versus Young's modulus (f_f, E_f) and (b) Young's modulus versus ultimate strain (E_f, ε_{fu}).

Table 5
Statistical values for the Anderson-Darling goodness of fit test for each percentile and distribution.

Percentile	Normal	Log-normal	Weibull
20%	0.050	0.068	0.064
25%	0.342	0.366	0.333
30%	0.894	0.941	0.817
35%	2.518	2.658	2.154
40%	4.160	4.429	3.404
100%	5.453	5.485	9.897

recommended for reliability analysis. The following pairs were considered: (i) tensile strength and ultimate strain, (ii) tensile strength and Young's modulus, and (iii) Young's modulus and ultimate strain.

A linear regression analysis was firstly performed between tensile strength and ultimate strain without constraints. Results showed high correlation between these two properties (R^2 = 0.75) as illustrated in Fig. 9a. Additionally, the residual standard deviation related with the uncertainty of the proposed model was 0.062%, which means that a probabilistic model could indeed describe the correlation between the two mechanical parameters. The corresponding model was defined as follows:

$$\varepsilon_{fu} = 0.17 + 0.0005014 f_f + 0.0618 Z(\%), \quad (18)$$

where f_f is the tensile strength in MPa, ε_{fu} is the ultimate strain and $Z \sim N(0,1)$.

Based on the results above, a second correlation analysis was performed by constraining the linear relation to the origin. The results and observations were quite similar, as shown in Fig. 9b. The latter model had a standard deviation of 0.063% and was defined by the following expression:

$$\varepsilon_{fu} = 0.0005646 f_f + 0.0633 Z(\%). \quad (19)$$

The last expression can be recommended in practice to relate the two expressions, since it provides good results and is relatively simple. It should be mentioned that such result shows that the ultimate strain and tensile strength are highly correlated variables. However, since both are not deterministic, the numerical value in

Table A1
Details of coupon samples.

Cross-section (mm^2)	Area (mm^2)	Sample size (#)
50 × 1.2	60	85
50 × 1.4	70	422
60 × 1.4	8.4	54
80 × 1.2	96	110
80 × 1.4	112	122
90 × 1.4	126	41
100 × 1.2	120	144
100 × 1.4	140	192
120 × 1.2	144	43
120 × 1.4	168	155

the equation should not be directly compared with the inverse ratio of the Young's modulus – although both are similar given the linear nature of the correlation found.

It should be highlighted that from this study, the tensile strength and Young's modulus were found to have a small correlation – see representation in Fig. 10a. Similar observation was also found between the Young's modulus and ultimate strain (Fig. 10b). This suggests that the variables could be considered as independent in both situations.

6. Conclusions

This manuscript presented a statistical analysis on mechanical properties of prefabricated CFRP laminates obtained from a large set of tests. Results showed that the Weibull distribution can be adopted to model the Young's modulus, the ultimate strain and the tensile strength of CFRP laminates. Furthermore, it was shown that the statistical characterisation of the CFRP should be carried out giving particular attention to the tail region. In fact, although an overall good fit of any selected distribution can be achieved in most cases, the approximation obtained in the tail region is not acceptable.

A low variability in the mechanical properties was also observed in this study, which is most significant in terms of structural safety. The lowest coefficient of variation is found for the Young's modulus, with the characteristic values from experimental data and proposed distributions being also very similar.

The correlation analysis between mechanical properties demonstrated that a probabilistic model relating the tensile strength and ultimate strain can be proposed. However, despite the strain, stress and Young's modulus being related by the Hooke's law in the linear elastic region, no probabilistic model could be proposed between tensile strength or ultimate strain and Young's modulus. In fact, these pairs of variables can be considered as independent.

As a final note, it should be mentioned that the distributions given in this paper can be used for carrying out reliability analyses aimed at proposing partial safety factors for the future revision of design codes.

Acknowledgements

The authors acknowledge the data provided by S&P Clever Reinforcement Ibérica. Sara Gomes would like to acknowledge the research grant from the Portuguese Science and Technology Foundation (SFRH/BD/76345/2011) and D. Dias-da-Costa would like to acknowledge the support from the Australian Research Council through its Discovery Early Career Researcher Award (DE 150101703) and from the Faculty of Engineering and Information Technologies, The University of Sydney, under the Faculty Research Cluster Program.

Appendix A: Sample distribution

Table A-1 provides the sample size and geometrical data for the 1368 coupon samples studied in this paper.

References

[1] M.B. Leeming, L.C. Hollaway, Strengthening of Reinforced Concrete Structures, Woodhead Publishing Limited, 1999.
[2] S.A. Hadigheh, R.J. Gravina, S. Setunge, Influence of the processing techniques on the bond characteristics in externally bonded joints- Experimental and analytical investigations, Compos. Constr. 20 (2016) 1–13.
[3] S.A. Hadigheh, R.J. Gravina, Generalization of the interface law for different FRP processing techniques in FRP-to-concrete bonded interfaces, Compos. Part B: Eng. 91 (2016) 399–407.
[4] V.M. Karbhari, Materials considerations in FRP rehabilitation of concrete structures, J. Mater. Civil Eng. 13 (2001) 90–97.
[5] A. Mirmiran, M. Shahawy, M. Samaan, H.E. Echary, J.C. Mastrapa, O. Pico, Effect of column parameters on FRP-confined concrete, J. Compos. Constr. 2 (1998) 175–185.
[6] A. Khalifa, W.J. Gold, A. Nanni, M.I. Abdel Aziz, Contribution of externally bonded FRP to shear capacity of RC flexural members, J. Compos. Constr. 2 (1998) 195–202.
[7] S.A. Hadigheh, R.J. Gravina, S. Setunge, Prediction of the bond-slip law in externally laminated concrete substrates by an analytical based nonlinear approach, Mater. Des. 66 (2015) 217–226.
[8] S.T. Smith, H. Zhang, Z. Wang, Influence of FRP anchors on the strength and ductility of FRP-strengthened RC slabs, Constr. Build. Mater. 49 (2013) 998–1012.
[9] CEB-FIB. FIB-Bulletin 14- Externally bonded FRP reinforcement for RC structures. Geneva, Switzerland: Fédération International du Béton (FIB); 2001. p. 130.
[10] TR-55. Design guidance for strenghening concrete structures using fibre composite materials. SOCIETY, C.(ed.); 2000.
[11] CNR. Guide for the design and construction of externally bonded FRP systems for strengthening existing structures. National Research Council, Advisory Committee on Technical Recommendations for Constructuion2001.
[12] ACI 440.2R-08. Guide for the design and construction of externally bonded FRP system for strengthening concrete structures. Michigan (USA): MCP 2005. ACI., 2008.
[13] B.R. Ellingwood, Toward load and resistance factor design for fiber-reinforced polymer composite structures, J. Struct. Eng. 129 (2003) 449–458.
[14] N. Wang, B.R. Ellingwood, A.H. Zureick, Reliability-based evaluation of flexural members strengthened with externally bonded fiber-reinforced polymer composites, J. Struct. Eng.. 136 (2010) 1151–1160.
[15] N. Plevris, T.C. Triantafillou, D. Veneziano, Reliability of RC members strengthened with CFRP laminates, J. Struct. Eng. 121 (1995) 1037–1044.
[16] A.M. Okeil, S. El-Tawil, M. Shahawy, Flexural reliability of reinforced concrete bridge girders strengthened with carbon fiber-reinforced polymer laminates, J. Bridge Eng. 7 (2002) 290–299.
[17] G. Monti, S. Santini, Reliability-based calibration of partial safety coefficients for fiber-reinforced plastic, J. Compos. Constr. 6 (2002) 162–167.
[18] R. Atadero, L. Lee, V.M. Karbhari, Consideration of material variability in reliability analysis of FRP strengthened bridge decks, Compos. Struct. 70 (2005) 430–443.
[19] R.A. Atadero, V.M. Karbhari, Calibration of resistance factors for reliability based design of externally-bonded FRP composites, Compos. Part B: Eng. 39 (2008) 665–679.
[20] A.M. Okeil, A. Belarbi, D.A. Kuchma, Reliability assessment of FRP-strengthened concrete bridge girders in shear, J. Compos. Constr. 17 (2013) 91–100.
[21] O. Ali, D. Bigaud, E. Ferrier, Comparative durability analysis of CFRP-strengthened RC highway bridges, Constr. Build. Mater. 30 (2012) 629–642.
[22] R.A. Atadero, V.M. Karbhari, Sources of uncertainty and design values for field-manufactured FRP, Compos. Struct. 89 (2009) 83–93.
[23] R.A. Atadero, Development of load and resistance factor design for FRP strengthening of reinforced concrete structures PhD Thesis, University of California, 2006.
[24] A.H. Zureick, R.M. Bennett, B.R. Ellingwood, Statistical characterization of fiber-reinforced polymer composite material properties for structural design, J. Struct. Eng. 132 (2006) 1320–1327.
[25] H.K. Jeong, R.A. Shenoi, Probabilistic strength analysis of rectangular FRP plates using Monte Carlo simulation, Comput. Struct. 76 (2000) 219–235.
[26] D.J. Lekou, T.P. Philippidis, Mechanical property variability in FRP laminates and its effect on failure prediction, Compos. Part B: Eng. 39 (2008) 1247–1256.
[27] B.R. Ellingwood, Acceptable risk bases for design of structures, Progress Struct. Eng. Mater. 3 (2001) 170–179.
[28] EN ISO 527-5, Plastics- Determination of Tensile Properties, Part 5: Test Conditions for Unidirectional Fibre-Reinforced Plastic Composites, European Committee for Standardization, 2009.
[29] M. Alqam, R.M. Bennett, A.H. Zureick, Three-parameter vs. two-parameter Weibull distribution for pultruded composite material properties, Compos. Struct. 58 (2002) 497–503.

[30] D.V. Lindley, Introduction to probability and statistics, Cambridge University Press, 1965.
[31] M. Havbro Faber, J. Köhler, Sorensen J. Dalsgaard, Probabilistic modeling of graded timber material properties, Struct. Safety 26 (2004) 295–309.
[32] J.F. Lawless, Statistical models and methods for lifetime data, Wiley, 1982.
[33] M. Stephens, R. D'Agostino, Goodness-of-fit Techniques, Marcel Dekker, 1986.
[34] R.J. Quantrill, L.C. Hollaway, The flexural rehabilitation of reinforced concrete beams by the use of prestressed advanced composite plates, Compos. Sci. Technol. 58 (1998) 1259–1275.
[35] T.C. Triantafillou, N. Deskovic, M. Deuring, Strengthening of concrete structures With prestressed fiber reinforced plastic sheets, Struct. J. 89 (1992) 235–244.